REGULAR ARTICLE

blood advances

Human peripheral blood DNAM-1^{neg} NK cells are a terminally differentiated subset with limited effector functions

Kimberley A. Stannard,[1] Sébastien Lemoine,[2] Nigel J. Waterhouse,[3] Frank Vari,[1,4] Lucienne Chatenoud,[2] Maher K. Gandhi,[4] Ludovic Martinet,[5,6] Mark J. Smyth,[1,7,*] and Camille Guillerey[1,7,*]

[1]Immunology in Cancer and Infection Laboratory, QIMR Berghofer Medical Research Institute, Herston, QLD, Australia; [2]INEM–Institut Necker Enfants Malades, INSERM U1151, Paris, France; [3]Flow Cytometry and Imaging, QIMR Berghofer Medical Research Institute, Herston, QLD, Australia; [4]University of Queensland Diamantina Institute, Translational Research Institute, Brisbane, QLD, Australia; [5]Cancer Research Center of Toulouse, INSERM Unité Mixte de Recherche 1037, Toulouse, France; [6]Institut Universitaire du Cancer, Toulouse, France; and [7]School of Medicine, The University of Queensland, Herston, QLD, Australia

Key Points

- The lack of DNAM-1 expression defines a new subset of mature NK cells in the human peripheral blood.
- DNAM-1^{neg} NK cells have limited killing activity and are poor producers of interferon-γ.

Natural killer (NK) cells are a heterogeneous population of innate lymphocytes whose potent anticancer properties make them ideal candidates for cellular therapeutic application. However, our lack of understanding of the role of NK cell diversity in antitumor responses has hindered advances in this area. In this study, we describe a new CD56^{dim} NK cell subset characterized by the lack of expression of DNAX accessory molecule-1 (DNAM-1). Compared with CD56^{bright} and CD56^{dim}DNAM-1^{pos} NK cell subsets, CD56^{dim}DNAM-1^{neg} NK cells displayed reduced motility, poor proliferation, lower production of interferon-γ, and limited killing capacities. Soluble factors secreted by CD56^{dim}DNAM-1^{neg} NK cells impaired CD56^{dim}DNAM-1^{pos} NK cell–mediated killing, indicating a potential inhibitory role for the CD56^{dim}DNAM-1^{neg} NK cell subset. Transcriptome analysis revealed that CD56^{dim}DNAM-1^{neg} NK cells constitute a new mature NK cell subset with a specific gene signature. Upon in vitro cytokine stimulation, CD56^{dim}DNAM-1^{neg} NK cells were found to differentiate from CD56^{dim}DNAM-1^{pos} NK cells. Finally, we report a dysregulation of NK cell subsets in the blood of patients diagnosed with Hodgkin lymphoma and diffuse large B-cell lymphoma, characterized by decreased CD56^{dim}DNAM-1^{pos}/CD56^{dim}DNAM-1^{neg} NK cell ratios and reduced cytotoxic activity of CD56^{dim}DNAM-1^{pos} NK cells. Altogether, our data offer a better understanding of human peripheral blood NK cell populations and have important clinical implications for the design of NK cell–targeting therapies.

Introduction

Natural killer (NK) cells are innate lymphoid cells that play important roles in the elimination of malignant or virally infected cells.[1] In addition to their cytotoxic functions, NK cells secrete cytokines and chemokines that contribute to the development of adaptive immune responses. NK cell activation is controlled by an array of receptors. Human NK cells express killer-cell immunoglobulin-like receptors (KIRs) that transmit negative signals upon binding to class I molecules of the major histocompatibility complex.[2] Conversely, natural cytotoxicity receptors (NKp30, NKp44, and NKp46) and NKG2D sense stress-induced molecules and contribute to NK cell activation. NK cell activity results from the integration of signals provided by these receptors as well as coreceptors, adhesion molecules, and cytokines.

Human NK cells are usually defined as CD3^{neg}CD56^{pos} cells and are divided into 2 main subsets: CD56^{bright} and CD56^{dim} NK cells.[3] In the peripheral blood, ~90% of NK cells are CD56^{dim}, but CD56^{bright} NK cells predominate in lymph nodes and most tissues.[4] CD56^{dim} NK cells express high

Submitted 28 December 2018; accepted 25 April 2019. DOI 10.1182/bloodadvances.2018030676.

*M.J.S. and C.G. contributed equally to this study.

For original data, please contact camille.guillerey@mater.uq.edu.au.

The full-text version of this article contains a data supplement.

levels of the Fcγ receptor III (CD16), whereas CD56^{bright} NK cells are CD16$^{dim/neg}$. Furthermore, CD56^{bright} cells are CD62L^{pos} and express high levels of the inhibitory receptor CD94/NKG2A but are KIR^{neg}, whereas CD56^{dim} NK cells are CD62L^{neg}, CD94/NKG2A^{low}, and KIR^{high}.[5] There is convincing evidence that CD56^{bright} NK cells are immature and differentiate into CD56^{dim} NK cells under cytokine stimulation.[6,7] CD56^{bright} NK cells are generally seen as an immunoregulatory subset characterized by its high production of cytokines such interferon-γ (IFN-γ), granulocyte-macrophage colony stimulating factor (GM-CSF), and tumor necrosis factor–α, whereas CD56^{dim} NK cells are endowed with high cytotoxic potential.[3] Although NK cell diversity expands far beyond CD56^{dim} and CD56^{bright} subsets,[8-10] the functional impact of this vast phenotypic diversity and the progeny relationship between NK cell subsets remain elusive.

DNAX accessory molecule-1 (DNAM-1, CD226) is an adhesion and costimulatory molecule known to promote NK cell cytotoxic activity and IFN-γ production upon binding to its ligands CD112 and CD155.[11] DNAM-1 shares its ligands with the inhibitory molecules TIGIT and CD96.[12] DNAM-1 has been involved in NK cell–mediated tumor immunosurveillance,[13-16] control of metastatic disease,[17] and defense against pathogens.[18,19] Importantly, DNAM-1 expression identifies 2 distinct NK cell functional subsets in mice, with DNAM-1^{neg} NK cells arising from DNAM-1^{pos} NK cells.[20] Although mouse DNAM-1^{pos} NK cells produce high levels of inflammatory cytokines, have enhanced interleukin-15 (IL-15) signaling, and proliferate vigorously, their DNAM-1^{neg} counterpart produces high amounts of macrophage inflammatory protein-1 (MIP-1) chemokines. In humans, DNAM-1 is expressed on the majority of peripheral blood NK cells, but bimodal DNAM-1 expression has been observed on lymphoid tissue–resident NK cells.[21] Several studies reported a reduction in DNAM-1 expression on NK cells isolated from patients with cancer.[22-26] Nevertheless, whether DNAM-1^{neg} human NK cells represent a distinct NK cell subset with specific functions has not yet been studied.

In the current study, we established that human peripheral blood DNAM-1^{neg} NK cells represent a distinct NK cell subset with a specific gene expression program. We showed that DNAM-1^{neg} NK cells arise from DNAM-1^{pos} NK cells and have limited effector functions. Moreover, proportions of DNAM-1^{neg} NK cells are increased in the blood of patients with lymphoma, highlighting the necessity of considering this subset when designing immunotherapies.

Materials and methods

Sample collection and study subjects

This study was approved by the Human Research Ethics committee at QIMR Berghofer and the Princess Alexandra Hospital, Brisbane. Buffy coat blood packs were collected from healthy volunteer blood donors through the Australian Red Cross Blood Service (Queensland, Australia). Samples from patients with Hodgkin lymphoma (HL) and diffuse large B-cell leukemia (DLBCL) and from age- and sex-matched healthy donors were collected pretreatment at the Princess Alexandra Hospital, Brisbane. All samples used in this study have been supplied with written informed consent.

Cell preparation and functional assays

NK cells were enriched from cryopreserved peripheral blood mononuclear cells (PBMCs) by negative selection using an automated separator (Miltneyi Biotec). NK cell subsets were purified by using flow cytometry (FACSAria II; BD Biosciences). Cells were cultured in complete RPMI 1640. The supplemental Methods present details regarding the NK cell functional assays.

Flow cytometry and cytokine detection

Cells were stained according to standard protocols (supplemental Table 1). Zombie yellow (BioLegend) was used to gate out dead cells. Isotype or fluorescence-minus-one controls were used to set positive staining gates. Intracellular staining was performed by using the BD intracellular staining kit (BD Biosciences). Cell apoptosis was measured by using the BD Annexin V Apoptosis Detection Kit. Data were acquired by using the LSR Fortessa IV (BD Biosciences) and analyzed with FlowJo software (Tree Star). Cytokines in the supernatant of in vitro cultures were analyzed by using cytometric bead array technology according to the manufacturer's instructions (BD Biosciences).

Live cell imaging and image analysis

NK cell motility and NK/target cell interactions were visualized by time-lapse microscopy with an Xcellence IX81 microscope (Olympus Corporation). Live cell images were taken at 40-second intervals over a 40- to 90-minute time period. Imaris version 8.2 software (Bitplane) was used to track live cells and generate motility data. Trajectory graphs were generated in Microsoft Excel using displacement data.

RNA sequencing

Details regarding RNA sequencing (RNAseq) are given in the supplemental Methods.

Telomere length measurement

The length of telomeric repeats was determined by quantitative flow–fluorescence in situ hybridization by using a telomere-specific, fluorescently labeled peptide nucleic acid probe according to the manufacturer's instructions (DakoCytomation).

Statistical analysis

Statistical analysis was performed by using Prism 6 software (GraphPad). Data were compared by using either 1-way or 2-way analysis of variance (ANOVA) with Tukey multiple comparison post hoc testing. $P < .05$ was considered significant. P values are depicted as $^{*}P < .05$, $^{**}P < .01$, $^{***}P < .001$, and $^{****}P < .0001$.

Results

Identification of a new NK cell subset characterized by the absence of DNAM-1 expression

To determine whether, similarly to mice,[20] distinct DNAM-1^{pos} and DNAM-1^{neg} NK populations exist in humans, we analyzed DNAM-1 expression on peripheral blood NK cells (CD3^{neg}CD56^{pos}) from 13 healthy donors. In agreement with previous reports,[25,27] most NK cells expressed DNAM-1 (Figure 1A; supplemental Figure 1A). However, although CD56^{bright} NK cells were exclusively DNAM-1^{pos}, a small population of DNAM-1^{neg} NK cells was detected within the CD56^{dim} subset. These CD56^{dim}DNAM-1^{neg} cells

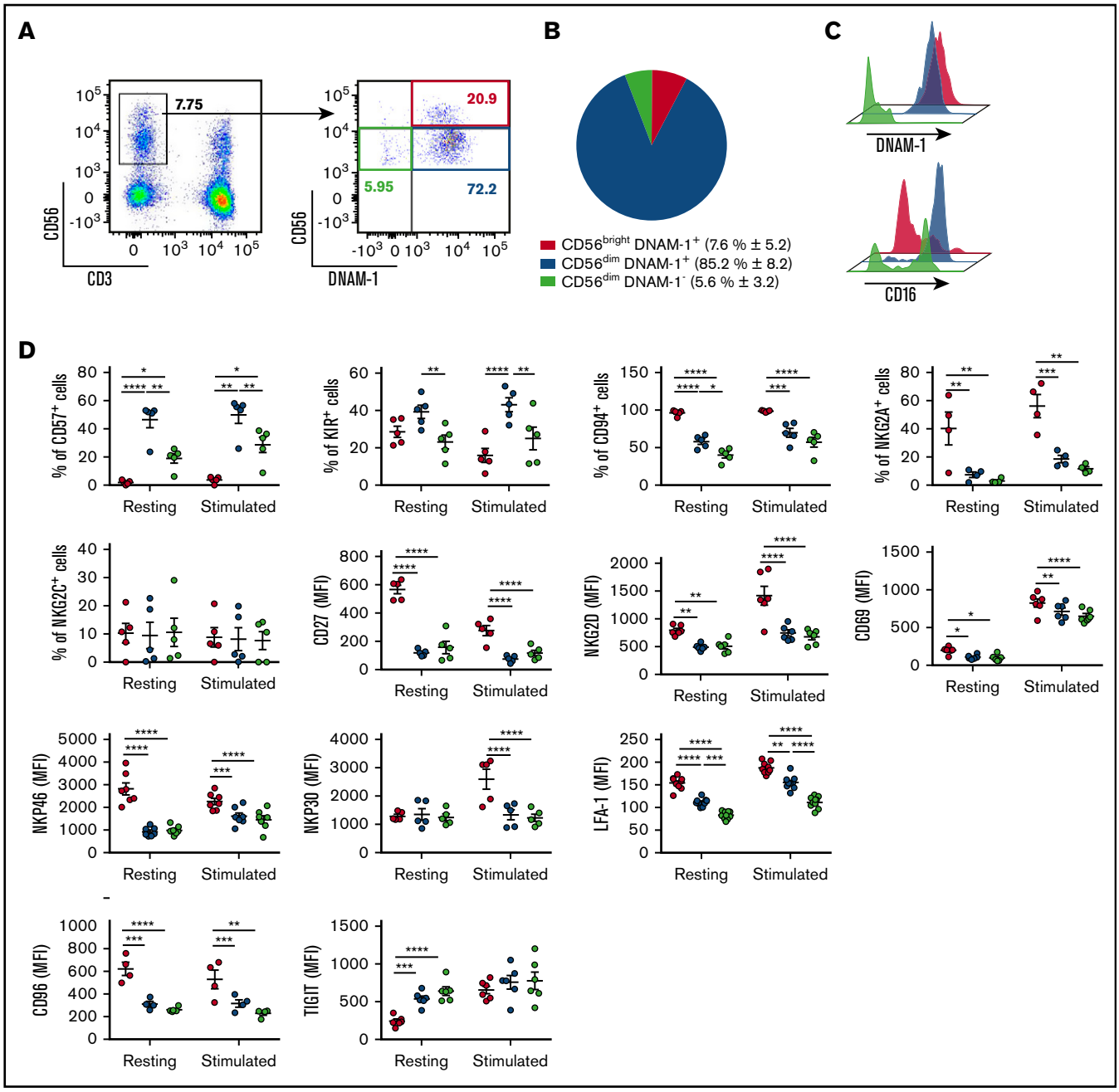

Figure 1. Low DNAM-1 expression defines a unique subset of CD56^{dim} NK cells displaying reduced expression of CD57, inhibitory KIRs, and LFA-1. (A) Representative fluorescence-activated cell sorter staining of healthy donor peripheral blood lymphocytes displaying the gating strategy used to identify NK cells (left) and CD56^{bright}DNAM-1^{pos}, CD56^{dim}DNAM-1^{pos}, and CD56^{dim}DNAM-1^{neg} NK cell subsets (right). Numbers show percentages of the gated populations. (B) Proportions of NK cell subsets defined as in panel A are shown as mean percentage ± standard deviation from 13 healthy donors. (C) Histograms showing DNAM-1 and CD16 expression on the 3 NK cell subsets defined as in panel A; CD56^{bright}DNAM-1^{pos} (red histogram), CD56^{dim}DNAM-1^{pos} (blue histogram), and CD56^{dim}DNAM-1^{neg} (green histogram). (D) Marker expression by NK cell subsets pre- and postovernight stimulation with IL-12 (10 ng/mL), IL-15 (100 ng/mL), and IL-18 (50 ng/mL) is shown as percentages of positive cells or mean fluorescence intensity (MFI). Single data points represent the mean value of duplicate wells. Data are shown as mean ± standard error of the mean (SEM) from 4 to 9 healthy donor samples and were analyzed by using a 2-way ANOVA followed by a Tukey multiple comparisons post hoc test. *$P < .05$; **$P < .01$; ***$P < .001$; ****$P < .0001$.

represented 5.6% ± 3.2% of the total peripheral blood NK cells (Figure 1B) and were detected in both fresh and cryopreserved samples (supplemental Figure 1B-C). The observations that CD56^{dim}DNAM-1^{neg} cells expressed both the NK cell–associated transcription factor Eomes and the NK cell linage marker CD122 and were negative for CD14 and CD19 confirmed their NK cell identity (supplemental Figure 1D-E). Hence, 3 human NK cell subsets were defined: CD56^{bright}DNAM-1^{pos}, CD56^{dim}DNAM-1^{pos}, and CD56^{dim}DNAM-1^{neg} NK cells. In agreement with previous reports,[3] CD56^{bright}DNAM-1^{pos} NK cells expressed low levels of

CD16, whereas CD56^{dim}DNAM-1^{pos} NK cells were mostly CD16^{pos}. Intriguingly, CD16 expression was bimodal on CD56^{dim}DNAM-1^{neg} NK cells (Figure 1C).

Overall, CD56^{dim}DNAM-1^{neg} NK cells appeared very similar to CD56^{dim}DNAM-1^{pos} NK cells: compared with CD56^{bright} NK cells, both CD56^{dim} subsets exhibited decreased expression levels of CD27, CD69, CD94, NKG2D, NKG2A, and natural cytotoxicity receptors (NKp30 and NKp46) (Figure 1D). CD96 and TIGIT also harbored similar expression patterns on DNAM-1^{pos} and DNAM-1^{neg} CD56^{dim} NK cells and were, respectively, decreased and increased compared with CD56^{bright} NK cells. However, expression levels of inhibitory KIRs were equivalent between CD56^{bright}DNAM-1^{pos} and CD56^{dim}DNAM-1^{neg} NK cells and were reduced compared with their CD56^{dim}DNAM-1^{pos} counterpart. Moreover, the maturation marker CD57 was expressed by one-half of CD56^{dim}DNAM-1^{pos} NK cells but only 20% to 30% of CD56^{dim}DNAM-1^{neg} NK cells. Finally, CD56^{dim}DNAM-1^{neg} NK cells expressed very low levels of the DNAM-1–associated adhesion molecule LFA-1.[28] These data identify a new CD56^{dim}DNAM-1^{neg} NK cell population that differs phenotypically from CD56^{dim}DNAM-1^{pos} NK cells by exhibiting lower expression of CD57 and KIRs.

CD56^{dim}DNAM-1^{neg} NK cells display reduced motility

DNAM-1 is an adhesion molecule[27] and might influence NK cell motility. We therefore investigated the migratory behavior of cytokine-activated NK cell subsets. We observed that DNAM-1^{pos} NK cells were elongated compared with the majority of DNAM-1^{neg} NK cells that appeared spherically symmetrical (Figure 2A). Compared with DNAM-1–expressing subsets, CD56^{dim}DNAM-1^{neg} NK cells displayed minimal motility and tended to move by involuntary drift (Figure 2B; supplemental Figure 2A-B). CD56^{bright}DNAM-1^{pos} and CD56^{dim}DNAM-1^{pos} NK cells were significantly faster (Figure 2C) and traveled longer tracks (Figure 2D) than CD56^{dim}DNAM-1^{neg} cells, even though no significant difference was observed regarding the displacement from origin (Figure 2E). Thus, CD56^{dim}DNAM-1^{neg} NK cells present an altered migratory behavior in vitro.

DNAM-1^{neg} NK cells exhibit limited proliferation and are poor producers of IFN-γ in response to cytokine stimulation

We assessed the proliferation of sorted NK cell subsets after 5 days of culture in the presence of IL-2 and IL-15 (Figure 3A). We observed that CD56^{bright} NK cells proliferated more than CD56^{dim} NK cells (as shown by Romagnani et al[7]); within the CD56^{dim} fraction, CD56^{dim}DNAM-1^{neg} NK cells exhibited reduced proliferation. We next measured IFN-γ production by using purified human NK cell subsets following in vitro stimulation with IL-12, IL-15, and IL-18. In agreement with previously published data,[3] higher percentages of IFN-γ–producing cells were observed within the CD56^{bright} NK cell subset compared with both CD56^{dim} subsets (Figure 3B). Interestingly, CD56^{dim}DNAM-1^{pos} NK cells were better IFN-γ producers than CD56^{dim}DNAM-1^{neg} NK cells. Further to this, we analyzed cytokine secretion in the culture supernatant of 6 purified NK cells subsets based on DNAM-1, CD56, and CD16 expression (gated as in supplemental Figure 3). CD56^{bright}CD16^{neg}DNAM-1^{pos} NK cells secreted more IFN-γ and GM-CSF than the other subsets (Figure 3C). CD56^{dim}CD16^{neg}DNAM-1^{pos} also secreted relatively high levels of IFN-γ and GM-CSF, in agreement with the idea that this population might represent an intermediate phenotype between CD56^{bright}CD16^{neg}DNAM-1^{pos} and CD56^{dim}CD16^{pos}DNAM-1^{pos} NK cells.[29] Importantly, both DNAM-1^{neg} subsets (CD56^{dim}CD16^{neg}DNAM-1^{neg} and CD56^{dim}CD16^{pos}DNAM-1^{neg}), similarly to CD56^{dim}CD16^{pos}DNAM-1^{pos} NK cells, were poor producers of IFN-γ and GM-CSF in response to cytokine stimulation. Finally, CD16 expression seemed to determine NK cell ability to produce MIP chemokines. Indeed, within the 3 main NK subsets described in this study (CD56^{bright}DNAM-1^{pos}, CD56^{dim}DNAM-1^{pos}, and CD56^{dim}DNAM-1^{neg}), CD16^{pos} cells always secreted more MIP-1α and MIP-1β than their CD16^{neg} counterpart. Taken as a whole, these data show very limited proliferation and IFN-γ secretion of CD56^{dim}DNAM-1^{neg} NK cells in response to cytokine stimulation.

DNAM-1^{neg} NK cells represent an immunomodulatory subset with limited killing capabilities

We investigated the response of DNAM-1^{neg} NK cells to receptor triggering through target cell stimulation. When incubated with the chronic myelogenous leukemia line K562, CD56^{dim}DNAM-1^{neg} NK cells expressed more CD107a than the other subsets (Figure 4A; supplemental Figure 4A). However, CD56^{dim}DNAM-1^{pos} NK cells killed K562 cells more effectively compared with both CD56^{bright}DNAM-1^{pos} cells and CD56^{dim}DNAM-1^{neg} NK cells (Figure 4B), in agreement with their high intracellular expression of granzyme B (supplemental Figure 4B). Analysis via time-lapse microscopy confirmed that CD56^{dim}DNAM-1^{pos} NK cells rapidly killed K562 cells, whereas CD56^{bright}DNAM-1^{pos} and CD56^{dim}DNAM-1^{neg} NK cells required a longer interaction time (Figure 4C). Thus, CD56^{dim}DNAM-1^{neg} NK cells respond to target cells, but this action does not translate to target cell killing.

We explored the possibility that this CD56^{dim}DNAM-1^{neg} population might have a regulatory function. To test this hypothesis, we performed a killing assay in which CD56^{dim}DNAM-1^{pos} NK cells were incubated with K562 target cells in the presence of conditioned medium (CM) from cytokine-stimulated CD56^{dim}DNAM-1^{neg} cultures (Figure 4D-E). The addition of CD56^{dim}DNAM-1^{neg} NK cell CM, but not heat-inactivated CM or CD56^{bright} NK cell CM, decreased CD56^{dim}DNAM-1^{pos} NK cell–killing capacity. These results suggest that soluble factors secreted by CD56^{dim}DNAM-1^{neg} NK cells may regulate the cytotoxic activity of CD56^{dim}DNAM-1^{pos} NK cells. Overall, our data indicate that the CD56^{dim}DNAM-1^{neg} NK cell subset presents limited effector functions but is endowed with immunomodulatory potential.

CD56^{dim}DNAM-1^{neg} NK cells constitute a mature NK cell subset with a specific gene signature

To better understand the relationship between CD56^{bright}DNAM-1^{pos}, CD56^{dim}DNAM-1^{pos} and CD56^{dim}DNAM-1^{neg} NK cell populations, we analyzed their gene expression profiles by using RNAseq. We confirmed that *Ncam1* (CD56) messenger RNA (mRNA) was highly expressed within the CD56^{bright} subset compared with the 2 CD56^{dim} subsets (Figure 5A). Interestingly, DNAM-1 downregulation in CD56^{dim}DNAM-1^{neg} NK cells was detected at the mRNA level, indicating that the absence of DNAM-1 expression on human CD56^{dim}DNAM-1^{neg} NK cells is not a consequence of internalization following ligand binding but likely results from repression of the *cd226* gene.

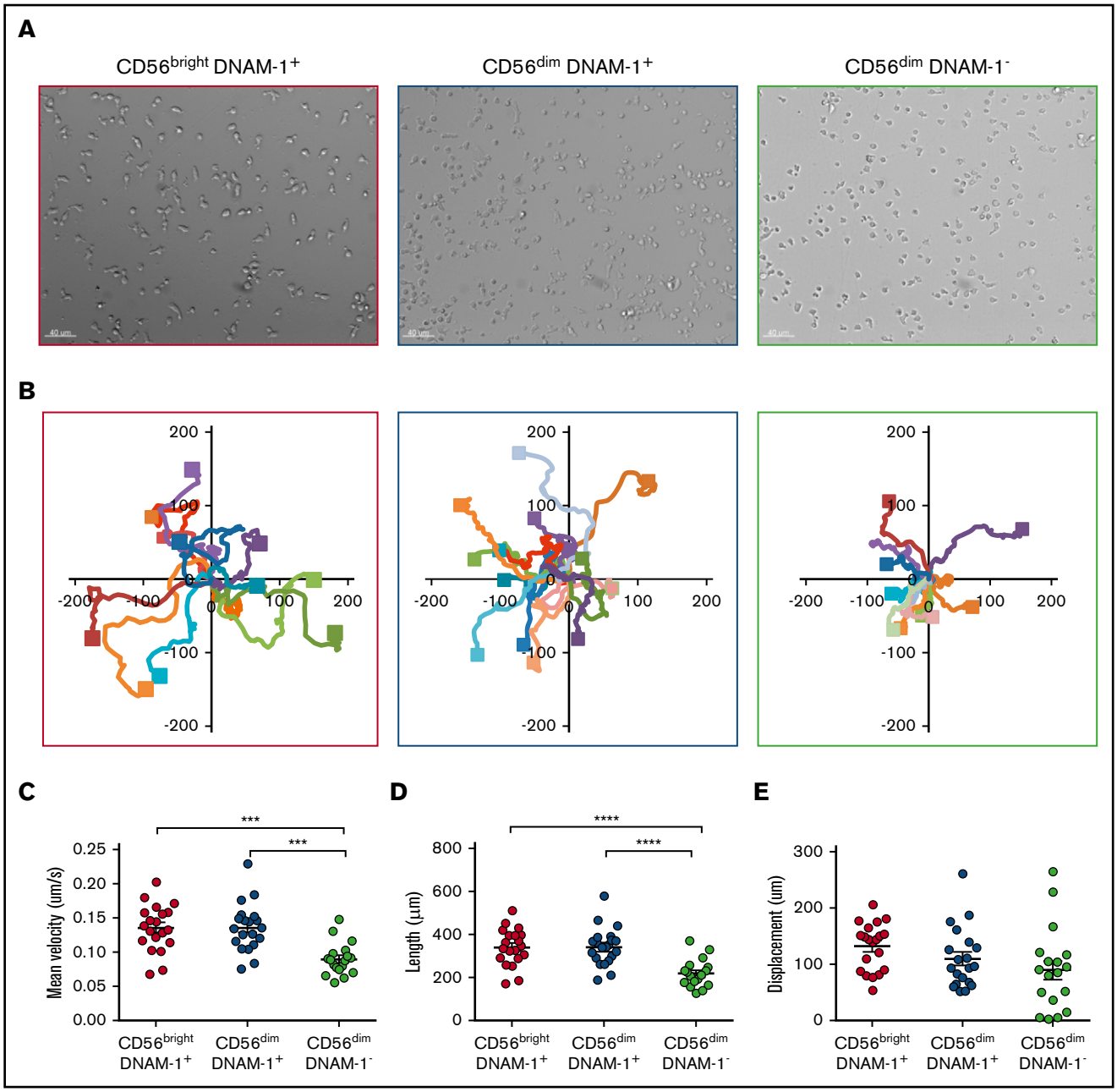

Figure 2. DNAM-1^{pos} NK cell subsets display more dynamic and deliberate migration behavior than CD56^{dim} DNAM-1^{neg} NK cells. CD56^{bright}DNAM-1^{pos}, CD56^{dim}DNAM-1^{pos}, and CD56^{dim}DNAM-1^{neg} NK cell subsets were fluorescence-activated cell sorter purified from healthy donor PBMCs. Cells were stimulated overnight with IL-12 (10 ng/mL), IL-15 (100 ng/mL), and IL-18 (50 ng/mL). Time-lapse microscopy was performed by using an Olympus Xcellence IX81 microscope controlled by Xcellence RT software. Images were taken every 40 seconds for 40 to 90 minutes. Images were collected by using a 20× LUCPlanFLN lens with 0.45 NA and Olympus F-View II camera. (A) Representative images. (B) Single-cell tracking map of NK cell trajectories. Mean velocity (C), length of tracks (D), and displacement from origin (E) of individual NK cells were calculated. Each data point represents 1 single randomly selected NK cell tracked over 40 minutes. Results are displayed as the mean ± SEM of at least 6 representative time-lapse videos obtained from 3 independent experiments. Data were analyzed by using a 1-way ANOVA followed by a Tukey multiple comparisons post hoc test. ***$P < .001$; ****$P < .0001$.

Unsupervised hierarchical clustering revealed that the 3 NK cell subsets clustered independently (Figure 5B), with both DNAM-1^{pos} subsets clustering together apart from CD56^{dim}DNAM-1^{neg} cells (Figure 5C). Analysis of the genes differentially expressed between the 3 NK cell subsets identified 6 groups of genes. In total, 2712 genes (groups B and F) were differentially expressed between DNAM-1^{pos} and DNAM-1^{neg} NK cells. Analysis of NK cell–related genes revealed high levels of *Kit* and *Il7r* mRNAs in CD56^{bright}DNAM-1^{pos} cells and high expression of *gzmb* (granzyme B) *in* CD56^{dim}DNAM-1^{pos} cells (Figure 5D), thereby confirming published observations.[4] Interestingly, although KIRs and *Tigit* mRNA expression matched our cytometry data, *cd96* mRNA was expressed on both DNAM-1^{pos}

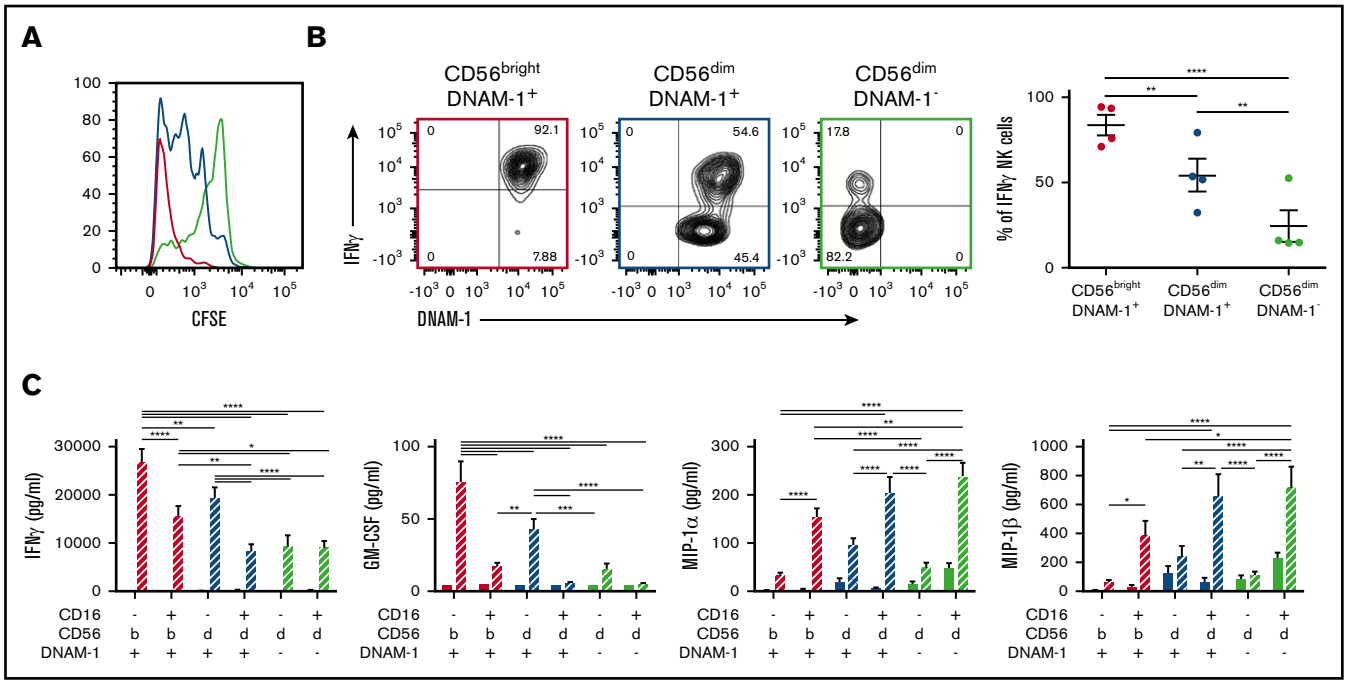

Figure 3. CD56^{dim} DNAM-1^{neg} NK cells proliferate poorly and produce limited amount of IFN-γ and granulocyte-macrophage colony-stimulating factor (GM-CSF) in response to cytokine stimulation. (A) CD56^{bright}DNAM-1^{pos} (red), CD56^{dim}DNAM-1^{pos} (blue), and CD56^{dim}DNAM-1^{neg} (green) NK cell subsets were purified from healthy donor PBMCs and stained with carboxyfluorescein diacetate succinimidyl ester (CFSE). The proliferation of NK cell subsets was assessed by measuring CFSE dilution after 5 days of culture with IL-2 (500 IU) and IL-15 (10 ng/mL). One representative histogram from 4 individual donors is displayed. (B) CD56^{bright}DNAM-1^{pos}, CD56^{dim}DNAM-1^{pos}, and CD56^{dim}DNAM-1^{neg} NK cell subsets were purified from healthy donor PBMCs. Intracellular IFN-γ production was assessed after overnight stimulation with IL-12 (10 ng/mL), IL-15 (100 ng/mL), and IL-18 (50 ng/mL). Representative fluorescence-activated cell sorting plots and cumulative data are shown. Each data point represents the mean percentage of IFN-γ^{+} NK cells obtained from culture duplicates; data are shown as mean ± SEM from 4 donor samples. (C) Healthy donor NK cells were purified into 6 subsets based on their expression of CD16 (+ or –), CD56 (bright [b] or dim [d]) and DNAM-1 (+ or –) and were cultured overnight with (striped fill pattern) or without (no fill pattern) stimulation with IL-12 (10 ng/mL), IL-15 (100 ng/mL), and IL-18 (50 ng/mL). Concentrations of indicated cytokines in the culture supernatant were analyzed by cytometric bead array. Data were normalized to reflect the relative cytokine/chemokine production per 10 000 cells and are presented as mean ± SEM of duplicate wells from 20 individual donors over 10 independent experiments. Data were analyzed with a 1-way (B) or 2-way (C) ANOVA followed by a Tukey multiple comparison post hoc test. *P <. 05; **P < .01; ***P < .001; ****P <.0001. No significant difference between subsets was found in the nonstimulated samples in panel C.

subsets, indicating that posttranscriptional mechanisms might regulate CD96 expression on the surface of CD56^{dim}DNAM-1^{pos} cells. *Tbx21* mRNA (encoding T-bet) was downregulated in the CD56^{dim}DNAM-1^{neg} subset, but these cells still expressed high levels of *Ifnγ* mRNA. CD56^{dim}DNAM-1^{neg} NK cells also expressed high levels of *Tnf* mRNA.

We analyzed selected genes encoding immunosuppressive molecules along with receptors for inflammatory cytokines and confirmed the high expression of cytokine receptors in the CD56^{bright}DNAM-1^{pos} subset (Figure 5E). The CD56^{dim}DNAM-1^{pos} subset expressed high levels of mRNAs encoding for subunits of the receptor to transforming growth factor β, a cytokine known to suppress NK cell activity.[30] CD56^{dim}DNAM-1^{neg} NK cells expressed high levels of prostaglandin E synthase mRNA, suggesting that the synthesis of prostaglandin E2[31] might contribute to the immunoregulatory activity of CD56^{dim}DNAM-1^{neg} NK cells.

Pathway network analyses confirmed the immaturity of CD56^{bright} cells, as pathways related to mitosis and Notch signaling[32] were preferentially expressed in this subset (supplemental Figure 5). Expression of pathways related to NK cell cytotoxicity, cell differentiation, receptor signaling, and intracellular signaling in the CD56^{dim}DNAM-1^{pos} subset suggested that these cells have been activated and have acquired killing capacities. CD56^{dim}DNAM-1^{neg} NK cells also appeared as a mature/activated subset that expressed pathways related to receptor/intracellular signaling. However, in contrast to CD56^{dim}DNAM-1^{pos} cells, pathways specific to this subset emphasized binding, either through cell adhesion or binding to immune compounds (immunoglobulins). Very interestingly, pathways related to inflammation (eg, inflammatory/immune response, cytokine/chemokine signaling, response to oxygen-containing compounds) were specifically expressed in CD56^{dim}DNAM-1^{neg} cells, suggesting that CD56^{dim}DNAM-1^{neg} NK cells might emerge in inflammatory conditions. Taken as a whole, these data established that CD56^{bright}DNAM-1^{pos}, CD56^{dim}DNAM-1^{pos}, and CD56^{dim}DNAM-1^{neg} NK cells represent 3 distinct NK cell subsets with different gene expression programs.

CD56^{dim}DNAM-1^{neg} NK cells constitute a subset of terminally differentiated NK cells

To assess the developmental relationship between CD56^{bright}DNAM-1^{pos}, CD56^{dim}DNAM-1^{pos}, and CD56^{dim}DNAM-1^{neg} NK cells, these subsets were purified from healthy donor PBMCs and cultured for 4 days in the presence of IL-2 only or a combination

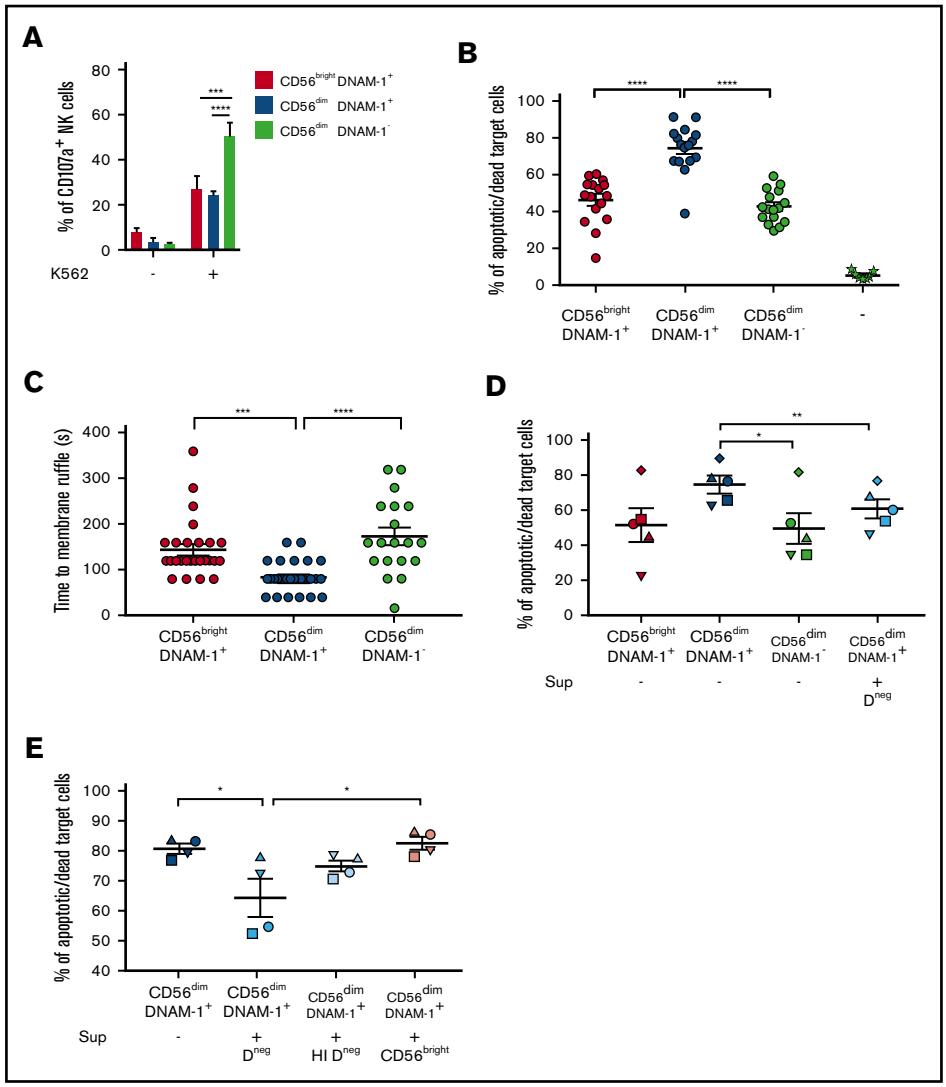

Figure 4. CD56^{dim} DNAM-1^{neg} NK cells present poor killing capabilities and downregulate the killing activity of CD56^{dim} DNAM-1^{pos} NK cells. (A) NK cells were enriched from PBMCs by Ficoll density gradient centrifugation followed by magnetic bead negative cell selection. K562 target cells were added to wells containing total NK cells in a 10:1 effector:target ratio. After 4 hours, cells were stained and analyzed for degranulation by quantifying the percentages of CD107a-positive cells after gating on CD56^{bright}DNAM-1^{pos} (red), CD56^{dim}DNAM-1^{pos} (blue), or CD56^{dim}DNAM-1^{neg} (green) NK cell subsets. Results are shown as percentages of positive cells ± SEM from 8 individual healthy donors, pooled from 2 independent experiments. (B-E) Fluorescence-activated cell sorting NK cell subsets were stimulated overnight in IL-12 (10 ng/mL), IL-15 (100 ng/mL), and IL-18 (50 ng/mL) and added to wells containing K562 target cells in a 10:1 effector:target ratio. (B) After 4 hours of culture, cytotoxicity of NK cell subsets against K562 target cells was quantified by flow cytometry with dead target cells identified as carboxyfluorescein diacetate succinimidyl ester (CFSE)^{neg} Annexin V/propidium iodide (PI)^{pos}. Target cells alone were used as control (–). Data are presented as mean ± SEM of percentages of Annexin V$^+$ and/or PI$^+$ target cells from 8 individual donors run in duplicate. Each dot represents one technical replicate. Data were pooled from 5 independent experiments. (C) The conjugation time between NK cells and target cells leading to target cell death was analyzed by using time-lapse microscopy. Time to membrane ruffle corresponds to the time (in seconds) between initial cell contact between the NK cell and the target cell and the first sign of target cell membrane ruffle. Results are shown as mean ± SEM from 20 to 30 individual NK cell:target cell conjugations pooled from at least 6 time-lapse videos obtained from 3 independent experiments. (D-E) Cytotoxicity of NK cell subsets was assessed as in panel B, but cells were cultured with (+) or without (–) supernatant from CD56^{dim}DNAM-1^{neg} (D^{neg}), heat-inactivated CD56^{dim}DNAM-1^{neg} (HI D^{neg}), or CD56^{bright}DNAM-1^{pos} (CD56^{bright}) NK cells that had been stimulated overnight in IL-12 (10 ng/mL), IL-15 (100 ng/mL), and IL-18 (50 ng/mL). Each graph shows the mean ± SEM of percentages Annexin V$^+$ and/or PI$^+$ target cells from 4 individual donors pooled from 2 independent experiments. Individual dots represent the mean value of duplicate wells for 1 donor. Data obtained from 1 individual donor are depicted with the same symbol. Data were analyzed by 2-way (A) or 1-way ANOVA without pairing (B-C) or a 1-way ANOVA with pairing (D-E) followed by a Tukey multiple comparison post hoc test. *$P < .05$; **$P < .01$; ***$P < .001$; ****$P < .0001$.

of IL-12, IL-15, and IL-18 (Figure 6A-B; supplemental Figure 6A). In both conditions, CD56^{bright}DNAM-1^{pos} NK cells gave rise to CD56^{dim}DNAM-1^{pos} NK cells and a minority of CD56^{dim}DNAM-1^{neg} NK cells. The appearance of CD56^{bright}DNAM-1^{pos} cells in CD56^{dim}DNAM-1^{pos} NK cell cultures in the presence of IL-2 might reflect CD56 upregulation after activation.[33] Importantly, a CD56^{dim}DNAM-1^{neg} NK cell population emerged in CD56^{dim}DNAM-1^{pos} NK cell cultures, suggesting that CD56^{dim}DNAM-1^{neg} NK

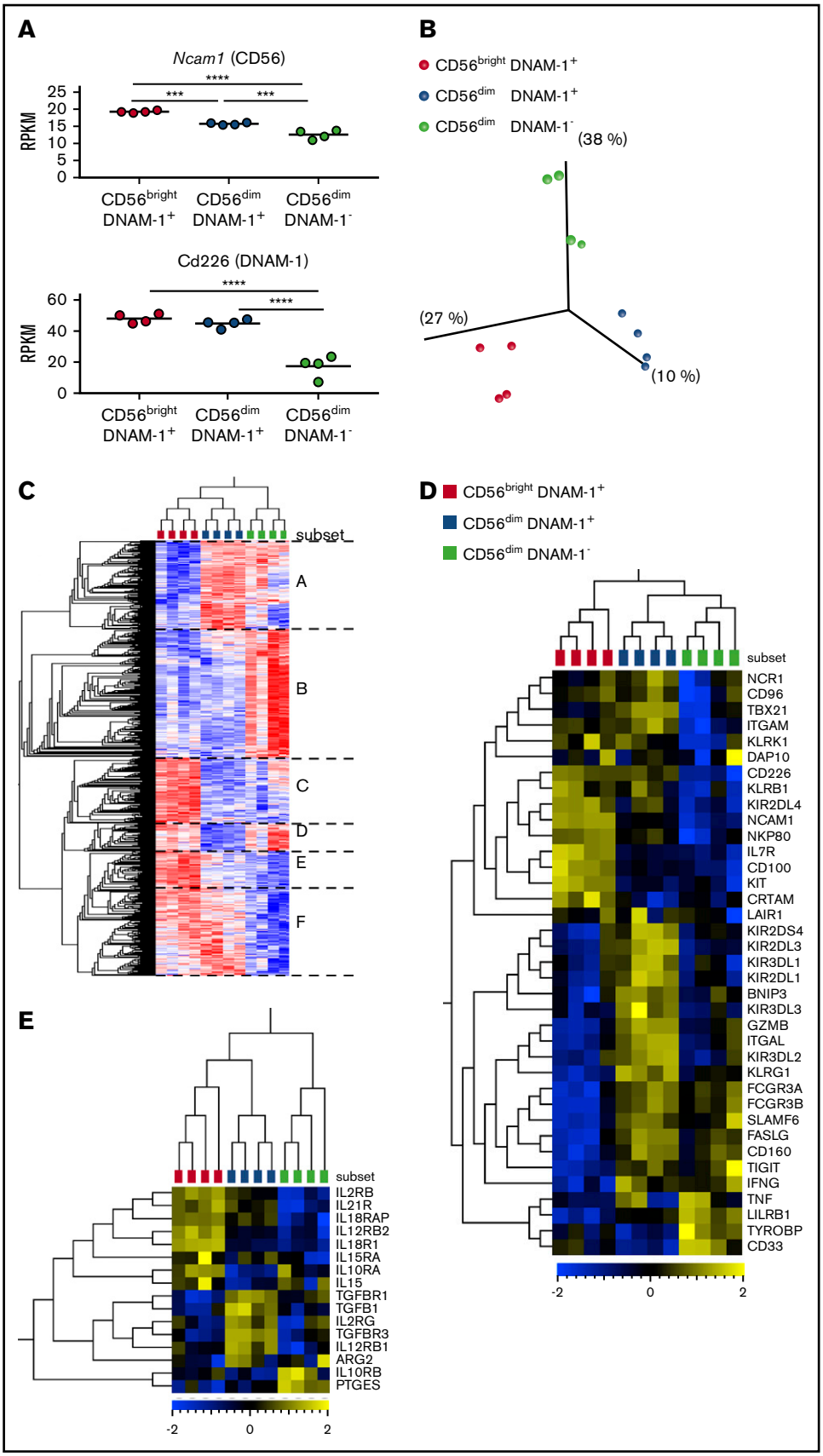

Figure 5. CD56^{bright} DNAM-1^{pos}, CD56^{dim} DNAM-1^{pos}, and CD56^{dim} DNAM-1^{neg} NK cell populations display distinct gene expression profiles. CD56^{bright}DNAM-1^{pos}, CD56^{dim}DNAM-1^{pos}, and CD56^{dim}DNAM-1^{neg} NK cell subsets were purified from healthy donor PBMCs, and their gene expression profiles were analyzed by using RNAseq. Four independent samples, each one consisting of NK cell mRNAs pooled from 10 to 20 donors, were analyzed for each population. (A) Relative expression of *Ncam1* and *Cd226* mRNAs in reads per kilobase million (RPKM). Data were analyzed with a 1-way ANOVA followed by a Tukey multiple comparison post hoc test. (B) Unsupervised principal component analysis revealed 3 clusters corresponding to the 3 NK cell populations (Benjamini-Hochberg corrected *P* value, q = 0.05). (C) Heat map and hierarchical clustering of the most differentially expressed genes between the 3 populations (q = 0.05). Genes can be divided into 6 groups (A-F) according to their pattern of expression. (D) Heat map displaying selected NK cell-related genes. (E) Heat map displaying selected genes related to inflammation and immunosuppression. ***$P < .001$; ****$P < .00001$.

cells derive from the CD56^{dim}DNAM-1^{pos} subset. Of note, the lower proliferative capacity of CD56^{dim}DNAM-1^{neg} NK cells excludes the possibility that a few contaminant CD56^{dim}DNAM-1^{neg} cells may have overgrown in these cultures. Finally, the vast majority of purified CD56^{dim}DNAM-1^{neg} NK cells conserved a stable phenotype, indicating that this subset represents a terminally differentiated stage that does not convert into any of the 2 other NK cell subsets. Of note, the pattern of expression of KIRs and CD57 in the 3 populations obtained postculture matched the phenotypes shown in Figure 1 (supplemental Figure 6B-C).

Telomere shortening is a process usually associated with cell replication, and terminally differentiated/memory lymphocyte subsets harbor shorter telomeres.[7] Although no significant difference was observed, CD56^{bright}DNAM-1^{pos} cells had the longest telomeres, whereas CD56^{dim}DNAM-1^{neg} had reduced telomeres (Figure 6C). When analyzing NK cell apoptosis in 2 different assays, we found that CD56^{dim}DNAM^{neg} NK cells were more resistant than the other subsets to cytokine starvation (Figure 6D), whereas a high proportion of CD56^{dim}DNAM-1^{neg} NK cells underwent apoptosis when cultured with inflammatory cytokines (Figure 6E). Taken as a whole, these results support a linear maturation pathway in which CD56^{bright}DNAM-1^{pos} NK cells differentiate into CD56^{dim}DNAM-1^{pos} NK cells that finally lose DNAM-1 expression to become CD56^{dim}DNAM-1^{neg} NK cells.

Proportions of CD56^{dim}DNAM-1^{pos} and CD56^{dim}DNAM-1^{neg} cell subsets are altered in the peripheral blood of patients with hematologic malignancies

We analyzed NK cell populations in the peripheral blood of a cohort of patients diagnosed with HL or DLBCL. Total NK cell percentages were reduced in the blood of patients with lymphoma compared with healthy donors (Figure 7A-B). This finding might be explained by a dramatic reduction of CD56^{dim}DNAM-1^{pos} NK cells in these patients (Figure 7C). In patients with DLBCL, decreased percentages in CD56^{dim}DNAM-1^{pos} NK cells among the whole NK cell population were associated with increased percentages in CD56^{dim}DNAM-1^{neg} NK cells; a similar trend, albeit not significant, was observed in patients with HL. Overall, the ratio of CD56^{dim}DNAM-1^{pos} NK cells over CD56^{dim}DNAM-1^{neg} NK cells was significantly reduced in both HL and DLBCL patients (Figure 7D). Marker analysis on the 3 NK cell populations revealed additional phenotypic alterations of NK cells in HL and DLBCL patients (supplemental Figure 7). An in vitro cytotoxicity assay against K562 target cells confirmed the limited killing capacity of CD56^{bright}DNAM-1^{pos} and CD56^{dim}DNAM-1^{neg} NK cells and indicated that the killing capacity of these 2 subsets was equivalent between healthy donors and patients with lymphoma (Figure 7E). Strikingly, the cytotoxic activity of CD56^{dim}DNAM-1^{pos} cells was decreased in patients with HL and DLBCL.

Discussion

We have identified a minor population of terminally differentiated NK cells that are characterized by a lack of DNAM-1 expression. This study expands to humans our previous findings that DNAM-1 expression patterns distinguish 2 mouse NK cell subsets with specific functions and gene expression profiles.[20]

The question of subset correspondence between mouse and human NK cells has recently been addressed by Crinier et al,[10] who used single-cell RNAseq to identify 2 NK cell subsets (NK1 and NK2) conserved across organs and species. The direct comparison of NK1 and NK2 signatures with our gene expression data set confirmed the validity of our RNAseq analysis, with CD56^{bright}DNAM-1^{pos} and CD56^{dim}DNAM-1^{pos} NK cells overexpressing the NK2 and NK1 signatures, respectively (supplemental Figure 8A-B). Interestingly, there was no correspondence between CD56^{dim}DNAM-1^{neg} NK cells and any of the blood or spleen subsets defined by Crinier et al, indicating that CD56^{dim}DNAM-1^{neg} NK cells constitute a new NK cell subset. We suggest that, in both mouse and human, DNAM-1 expression might allow the definition of alternative NK cell subsets that do not fall into the NK1/NK2 categories. Using the published mouse DNAM-1^{neg} NK cell signature,[20] we have defined a 6-gene DNAM-1^{neg} NK cell signature conserved across species (supplemental Figure 8C).

In addition to a specific gene signature, human DNAM-1^{neg} NK cells share several functional characteristics with their mouse counterpart: they arise from DNAM-1^{pos} NK cells, they display limited proliferative capacity, and they are poor producers of IFN-γ and GM-CSF. However, this report also highlights differences between the 2 species. Although DNAM-1^{neg} NK cells account for approximately one-half of mouse splenic NK cells,[20] DNAM-1^{neg} NK cells represent a minor population in the human peripheral blood. In mice, DNAM-1^{neg} NK cells are high producers of MIP chemokines.[20] By contrast, we found that in humans, MIP-producing NK cells are defined by the expression of CD16, regardless of whether they express DNAM-1. Finally, mouse DNAM-1^{pos} and DNAM-1^{neg} NK cell subsets display equivalent cytotoxic activity,[20] whereas in humans, CD56^{dim}DNAM-1^{pos} NK cells are much more potent killers than CD56^{dim}DNAM-1^{neg} NK cells.

The consensus that conventional NK cells originate via a linear differentiation model has been challenged by some research suggesting that CD56^{bright} and CD56^{dim} NK cells might belong to different lineages.[34] Our in vitro differentiation experiments confirm the well-accepted linear model of NK cell maturation and add an additional step: immature CD56^{bright} NK cells give rise to CD56^{dim}DNAM-1^{pos} NK cells that ultimately become CD56^{dim}DNAM-1^{neg} NK cells. In agreement of the concept of a progressive maturation program, we identified a group of genes (Figure 5C, cluster E) showing high expression in CD56^{bright} NK cells, moderate expression in CD56^{dim} DNAM-1^{pos} cells, and low expression in CD56^{dim}DNAM-1^{neg}. Nevertheless, we did not completely rule out the possibility that some CD56^{dim}DNAM-1^{neg} NK cells might directly arise from CD56^{bright} NK cells. In this regard, the low percentage of KIR^{+} cells and the common gene expression program (Figure 5C, cluster D) shared by CD56^{bright}DNAM-1^{pos} and CD56^{dim}DNAM-1^{neg} NK cells might be seen as an indication of a differentiation pathway independent from CD56^{dim}DNAM-1^{pos} NK cells.

Our data indicate that CD56^{dim}DNAM-1^{neg} NK cells are terminally differentiated cells: their phenotype remains stable upon cytokine stimulation, their telomeres are shorter than those of DNAM-1^{pos} NK cell subsets, and they are highly prone to apoptosis in inflammatory microenvironments but more resistant to cytokine withdrawal. However, surprisingly, only 20% to 30% of CD56^{dim}DNAM-1^{neg} NK cells express CD57, a marker commonly believed to mark

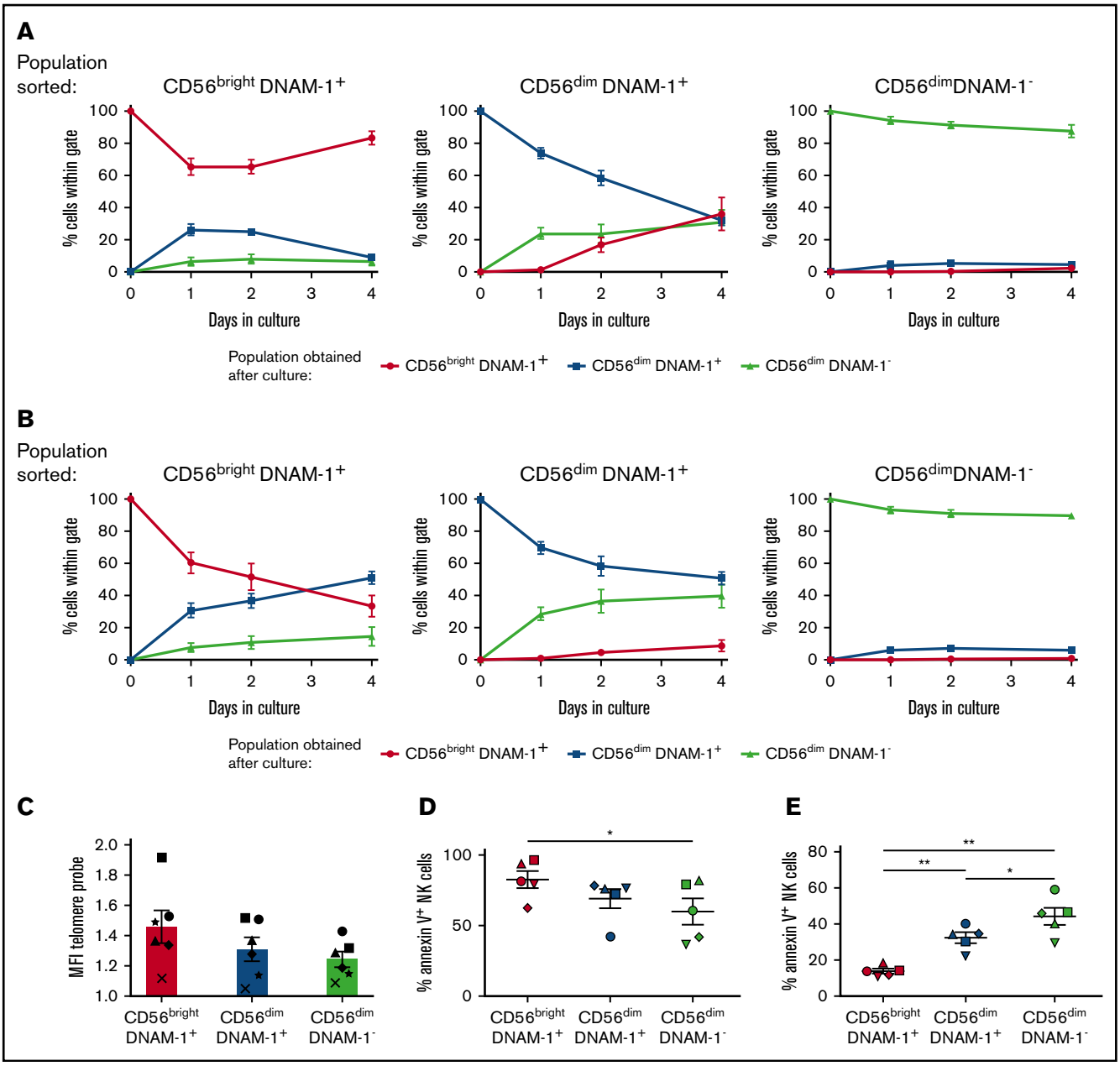

Figure 6. CD56^{dim} DNAM-1^{neg} NK cells are terminally differentiated. (A-B) CD56^{bright}DNAM-1^{pos}, CD56^{dim}DNAM-1^{pos}, and CD56^{dim}DNAM-1^{neg} NK cell subsets were purified from healthy donor PBMCs and cultured for 4 days in the presence of IL-2 (600 IU) (A) or IL-12 (10 ng/mL), IL-15 (100 ng/mL), and IL-18 (50 ng/mL) (B). At days 1, 2, and 4, NK cells were analyzed by using flow cytometry for surface expression of CD56 and DNAM-1. Results are displayed as the percentage of cells falling within CD56^{bright}DNAM-1^{pos}, CD56^{dim}DNAM-1^{pos}, or CD56^{dim}DNAM-1^{neg} gates. Data are shown as the mean ± SEM of duplicate wells from 5 individual donors pooled from 3 independent experiments. (C) Telomere length was determined by hybridization of a fluorescein isothiocyanate–labeled peptide nucleic acid probe to telomeric repeats in the DNA of NK cell subsets. For each NK cell subset, mean fluorescence intensity (MFI) values of the incorporated probe was normalized to K562 control cell fluorescence. Data are shown as mean ± SEM values obtained for 6 individual donors and are pooled from 3 independent experiments, with each symbol representing one individual donor. No significant difference was found by using a 1-way ANOVA on paired values. (D-E) Purified CD56^{bright}DNAM-1^{pos}, CD56^{dim}DNAM-1^{pos}, and CD56^{dim}DNAM-1^{neg} NK cells were cultured overnight in the absence (D) or presence (E) of IL-12 (10 ng/mL), IL-15 (100 ng/mL), and IL-18 (50 ng/mL). Apoptosis was determined by measuring Annexin V uptake by using flow cytometry. Data are shown as mean ± SEM from 5 individual donors. Individual dots represent the mean value of duplicate wells, with each symbol representing one individual donor. Data were analyzed by using a 1-way ANOVA on paired values followed by a Tukey multiple comparison post hoc test. *$P < .05$; **$P < .01$.

one of the final steps in NK cell maturation.[35-37] We propose that loss of DNAM-1 on both CD56^{dim}CD57^{pos} and CD56^{dim}CD57^{neg} NK cells represents an alternative maturation pathway that is associated with the acquisition of immunomodulatory functions. In this model, lower frequencies of CD57^{pos} cells within the DNAM-1^{neg} population might be explained by the reduced proliferative capacity of CD56^{dim}CD57^{pos} compared with CD56^{dim}CD57^{neg} cells.[35]

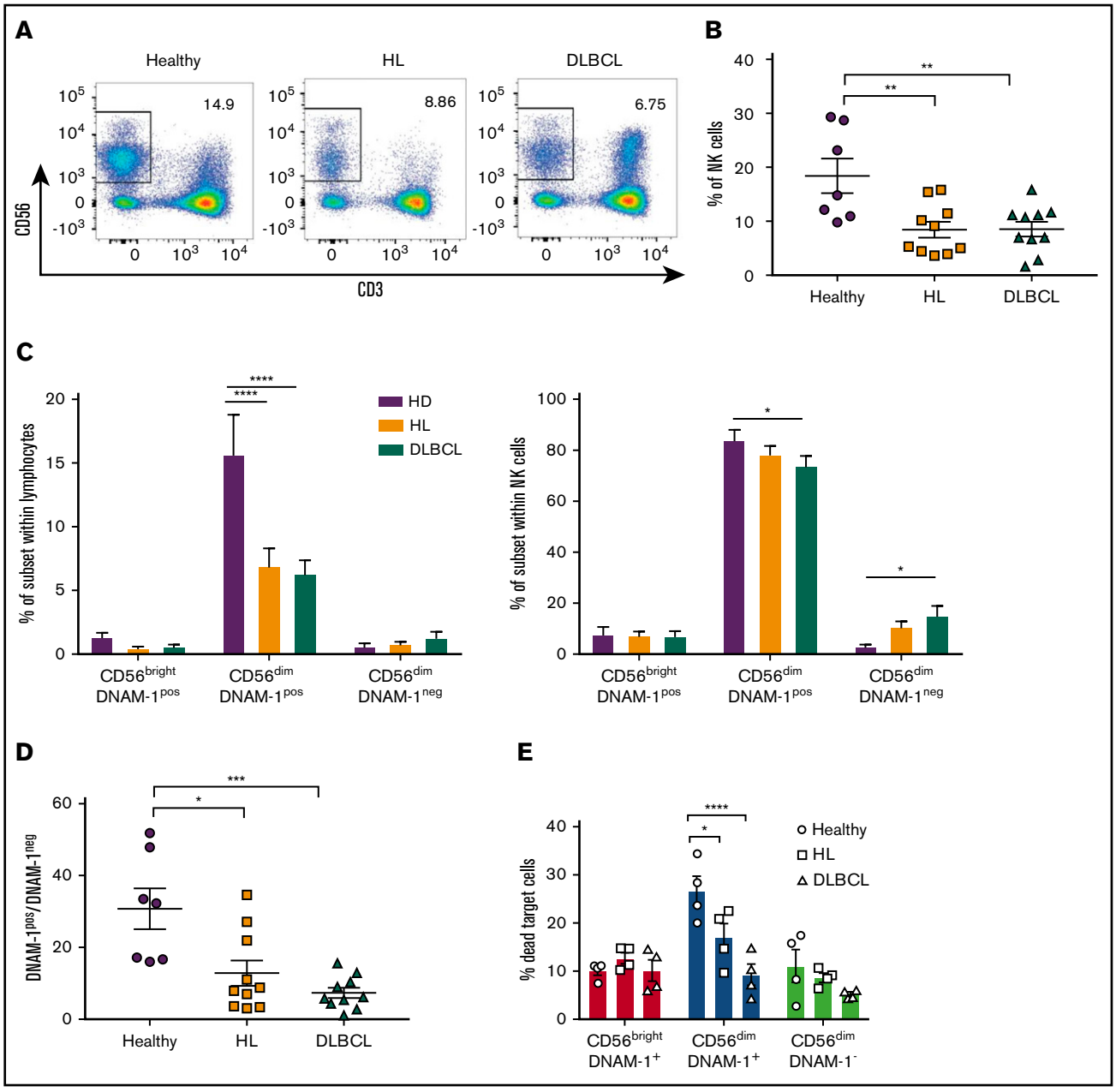

Figure 7. CD56^{dim} DNAM-1^{neg} NK cells are enriched in the peripheral blood of patients with hematologic malignancies. (A-B) NK cell proportions in peripheral blood of patients with HL or DLBCL compared with that of age- and sex-matched healthy control donors was determined via flow cytometry by gating on live CD3^{neg}CD56^{pos} NK cells. Representative fluorescence-activated cell sorter plots (A) and the mean ± SEM of duplicate wells from 7 to 10 individual donors (B) from each group are shown. (C) NK cell subset distribution was determined by flow cytometry from healthy donor and HL and DLBCL patient samples. Results are shown as the mean ± SEM of subset frequencies within the whole lymphocyte population (left) or the NK cell population (right). (D) Graph shows the ratio of CD56^{dim}DNAM-1^{pos} over CD56^{dim}DNAM-1^{neg} NK cell as mean ± SEM. (E) CD56^{bright}DNAM-1^{pos}, CD56^{dim}DNAM-1^{pos}, and CD56^{dim}DNAM-1^{neg} NK cell subsets were purified from healthy donor and HL or DLBCL PBMCs and stimulated overnight in IL-12 (10 ng/mL), IL-15 (100 ng/mL), and IL-18 (50 ng/mL). The following day, cells were added to wells containing K562 target cells in a 10:1 effector: target ratio. After 4 hours of culture, cytotoxicity of NK cell subsets against K562 target cells was measured by fluorescence-activated cell sorter staining for Annexin V/PI. Results are shown as mean ± SEM from 4 individual donors run in duplicate and pooled from 2 independent experiments. Individual dots represent the mean value of duplicate wells. Data were analyzed with a 1-way ANOVA (B,D) or a 2-way ANOVA (C,E) followed by a Tukey multiple comparison post hoc test. *$P < .05$; **$P < .01$; ***$P < .001$; ****$P < .0001$.

Intriguingly, increased CD107a expression observed on the membrane of K562-stimulated CD56^{dim}DNAM-1^{neg} NK cells did not translate into effective cytotoxicity. Several hypotheses can explain these contradictory results. First, the granules released by CD56^{dim}DNAM-1^{neg} NK cells may not contain the cytotoxic molecules required for target cell killing, a hypothesis supported by

the low expression of granzyme B of CD56^{dim}DNAM-1^{neg} NK cells. Alternatively, limited expression of LFA-1 on CD56^{dim}DNAM-1^{neg} cells coupled with the absence of DNAM-1–triggered inside-out LFA-1 signaling might have led to nonpolarized degranulation and limited killing of target cells.[38,39] Finally, similarly to what has been described for CD16,[40] NK cells might downregulate DNAM-1 after degranulation. In this case, higher percentage of CD107a^{+} cells within the CD56^{dim}DNAM-1^{neg} NK cell population might only be a consequence of their terminal differentiation from degranulating CD56^{dim}DNAM-1^{pos} NK cells.

Although CD56^{dim}DNAM-1^{neg} NK cells were limited in their ability to perform "classical" NK cell functions (ie, killing and IFN-γ secretion), our data indicate that these cells might represent an immunomodulatory subset. Although NK cells are known to play an immunoregulatory role in autoimmune diseases by the elimination of chronically activated immune cells,[41,42] this study is the first to indicate the self-regulation of NK cell cytotoxicity by the secretion of soluble factors from a terminally differentiated NK cell subset. The soluble factors implicated in this process remain to be identified. One main candidate is prostaglandin E2[31,43,44] as our RNAseq analysis identified increased expression of *ptges* in CD56^{dim}DNAM-1^{neg} NK cells.

We observed a profound decline in the ratio of CD56^{dim}DNAM-1^{pos} over CD56^{dim}DNAM-1^{neg} NK cell subsets in the blood of patients with HL and DLBCL that may be attributed to decreased numbers of CD56^{dim}DNAM-1^{pos} NK cells. In addition, we showed that, in patients with lymphoma, CD56^{dim}DNAM-1^{pos} NK cells present reduced cytotoxic activity. The decreased numbers and functionality of cytotoxic CD56^{dim}DNAM-1^{pos} NK cells associated with overrepresentation of potentially immunosuppressive CD56^{dim}DNAM-1^{neg} NK cells are likely to affect the efficacy of NK cell–targeting strategies in patients with lymphoma.

In conclusion, we identified a population of terminally differentiated CD56^{dim}DNAM-1^{neg} circulating human NK cells that are proportionally more represented in the blood of patients with HL and DLBCL. Because CD56^{dim}DNAM-1^{neg} NK cells are poor effectors and potentially immunosuppressive, this population is likely to affect the quality of ex vivo expanded NK cells for autologous cell transfer therapies. Future research should investigate whether depleting the CD56^{dim}DNAM-1^{neg} NK cells before culturing could improve the killing activity of patient NK cells and show better antilymphoma effect.

Acknowledgments

The authors thank the Flow Cytometry and Imaging Facility at QIMR Berghofer Medical Research Institute, the ACRF Centre for Comprehensive Biomedical Imaging, and the members of the Immunology in Cancer and Infection Laboratory for helpful suggestions and discussion. The authors acknowledge the specimen donors and thank the Red Cross Blood Service for their supply of buffy coats for this project.

C.G. was supported by a National Health and Medical Research Council (NHMRC) of Australia Early Career Fellowship (1107417), and M.J.S. was supported by an NHMRC Senior Principal Research Fellowship (1078671). This project was funded by a Priority-driven Collaborative Cancer Research Scheme project grant from Cancer Australia, Cure Cancer Australia, and Can Too (1122183) attributed to C.G., a project seed grant from QIMR Berghofer Medical Research Institute attributed to C.G., and an NHMRC Program Grant (1132519) attributed to M.J.S.

Authorship

Contribution: K.A.S., M.K.G., M.J.S., and C.G. were responsible for study conception and design; K.A.S. and N.J.W. were responsible for acquisition of data; K.A.S., S.L., N.J.W., M.J.S., and C.G. performed analysis and interpretation of data; K.A.S. and C.G. drafted the manuscript; S.L., F.V., L.C., M.K.G., L.M., and M.J.S. performed critical revisions and editing; and M.J.S. and C.G. were responsible for supervision.

Conflict-of-interest disclosure: M.J.S. has research agreements with Bristol-Myers Squibb, Tizona Therapeutics, and Aduro Biotech. M.K.G. has financial relationships with BMS (research grant), Celgene (research grant), MSD (advisory board), Janssen (advisory board), Gilead (honorarium and research grant), Roche (honoria and travel), and Amgen (honorarium). The remaining authors declare no competing financial interests.

The current affiliation for C.G. is Cancer Immunotherapies Laboratory, Mater Research Institute, The University of Queensland, Translational Research Institute, Woolloongabba, QLD, Australia.

ORCID profiles: M.K.G., 0000-0003-1000-5393; M.J.S., 0000-0001-7098-7240; C.G., 0000-0002-7917-2432.

Correspondence: Camille Guillerey, Cancer Immunotherapies Laboratory, Mater Research Institute, The University of Queensland, Translational Research Institute, Woolloongabba, QLD 4102, Australia; e-mail: camille.guillerey@mater.uq.edu.au; or Mark J. Smyth, QIMR Berghofer Medical Research Institute, 300 Herston Rd, Herston, QLD 4006, Australia; e-mail: mark.smyth@qimrberghofer.edu.au

References

1. Vivier E, Tomasello E, Baratin M, Walzer T, Ugolini S. Functions of natural killer cells. *Nat Immunol*. 2008;9(5):503-510.
2. Moretta L, Biassoni R, Bottino C, et al. Human NK cells and their receptors. *Microbes Infect*. 2002;4(15):1539-1544.
3. Cooper MA, Fehniger TA, Caligiuri MA. The biology of human natural killer-cell subsets. *Trends Immunol*. 2001;22(11):633-640.
4. Melsen JE, Lugthart G, Lankester AC, Schilham MW. Human circulating and tissue-resident CD56(bright) natural killer cell populations. *Front Immunol*. 2016;7:262.
5. Montaldo E, Del Zotto G, Della Chiesa M, et al. Human NK cell receptors/markers: a tool to analyze NK cell development, subsets and function. *Cytometry A*. 2013;83(8):702-713.

6. Huntington ND, Legrand N, Alves NL, et al. IL-15 trans-presentation promotes human NK cell development and differentiation in vivo. *J Exp Med*. 2009; 206(1):25-34.
7. Romagnani C, Juelke K, Falco M, et al. CD56brightCD16- killer Ig-like receptor- NK cells display longer telomeres and acquire features of CD56dim NK cells upon activation. *J Immunol*. 2007;178(8):4947-4955.
8. Freud AG, Mundy-Bosse BL, Yu J, Caligiuri MA. The broad spectrum of human natural killer cell diversity. *Immunity*. 2017;47(5):820-833.
9. Horowitz A, Strauss-Albee DM, Leipold M, et al. Genetic and environmental determinants of human NK cell diversity revealed by mass cytometry. *Sci Transl Med*. 2013;5(208):208ra145.
10. Crinier A, Milpied P, Escaliere B, et al. High-dimensional single-cell analysis identifies organ-specific signatures and conserved NK cell subsets in humans and mice. *Immunity*. 2018;49(5):971-986.e975.
11. de Andrade LF, Smyth MJ, Martinet L. DNAM-1 control of natural killer cells functions through nectin and nectin-like proteins. *Immunol Cell Biol*. 2014; 92(3):237-244.
12. Chan CJ, Martinet L, Gilfillan S, et al. The receptors CD96 and CD226 oppose each other in the regulation of natural killer cell functions. *Nat Immunol*. 2014;15(5):431-438.
13. Castriconi R, Dondero A, Corrias MV, et al. Natural killer cell-mediated killing of freshly isolated neuroblastoma cells: critical role of DNAX accessory molecule-1-poliovirus receptor interaction. *Cancer Res*. 2004;64(24):9180-9184.
14. Pende D, Spaggiari GM, Marcenaro S, et al. Analysis of the receptor-ligand interactions in the natural killer-mediated lysis of freshly isolated myeloid or lymphoblastic leukemias: evidence for the involvement of the Poliovirus receptor (CD155) and Nectin-2 (CD112). *Blood*. 2005;105(5):2066-2073.
15. Croxford JL, Tang ML, Pan MF, et al. ATM-dependent spontaneous regression of early Eμ-myc-induced murine B-cell leukemia depends on natural killer and T cells. *Blood*. 2013;121(13):2512-2521.
16. Guillerey C, Ferrari de Andrade L, Vuckovic S, et al. Immunosurveillance and therapy of multiple myeloma are CD226 dependent [published correction appears in *J Clin Invest*. 2015;125(7):2904]. *J Clin Invest*. 2015;125(5):2077-2089.
17. Chan CJ, Andrews DM, McLaughlin NM, et al. DNAM-1/CD155 interactions promote cytokine and NK cell-mediated suppression of poorly immunogenic melanoma metastases. *J Immunol*. 2010;184(2):902-911.
18. Nabekura T, Kanaya M, Shibuya A, Fu G, Gascoigne NR, Lanier LL. Costimulatory molecule DNAM-1 is essential for optimal differentiation of memory natural killer cells during mouse cytomegalovirus infection. *Immunity*. 2014;40(2):225-234.
19. Magri G, Muntasell A, Romo N, et al. NKp46 and DNAM-1 NK-cell receptors drive the response to human cytomegalovirus-infected myeloid dendritic cells overcoming viral immune evasion strategies. *Blood*. 2011;117(3):848-856.
20. Martinet L, Ferrari De Andrade L, Guillerey C, et al. DNAM-1 expression marks an alternative program of NK cell maturation. *Cell Reports*. 2015;11(1): 85-97.
21. Lugthart G, Melsen JE, Vervat C, et al. Human lymphoid tissues harbor a distinct CD69+CXCR6+ NK cell population. *J Immunol*. 2016;197(1):78-84.
22. Mamessier E, Sylvain A, Thibult ML, et al. Human breast cancer cells enhance self tolerance by promoting evasion from NK cell antitumor immunity. *J Clin Invest*. 2011;121(9):3609-3622.
23. Carlsten M, Norell H, Bryceson YT, et al. Primary human tumor cells expressing CD155 impair tumor targeting by down-regulating DNAM-1 on NK cells. *J Immunol*. 2009;183(8):4921-4930.
24. Peng YP, Xi CH, Zhu Y, et al. Altered expression of CD226 and CD96 on natural killer cells in patients with pancreatic cancer. *Oncotarget*. 2016;7(41): 66586-66594.
25. El-Sherbiny YM, Meade JL, Holmes TD, et al. The requirement for DNAM-1, NKG2D, and NKp46 in the natural killer cell-mediated killing of myeloma cells. *Cancer Res*. 2007;67(18):8444-8449.
26. Sanchez-Correa B, Gayoso I, Bergua JM, et al. Decreased expression of DNAM-1 on NK cells from acute myeloid leukemia patients. *Immunol Cell Biol*. 2012;90(1):109-115.
27. Shibuya A, Campbell D, Hannum C, et al. DNAM-1, a novel adhesion molecule involved in the cytolytic function of T lymphocytes. *Immunity*. 1996;4(6): 573-581.
28. Shibuya K, Lanier LL, Phillips JH, et al. Physical and functional association of LFA-1 with DNAM-1 adhesion molecule. *Immunity*. 1999;11(5):615-623.
29. Béziat V, Duffy D, Quoc SN, et al. CD56brightCD16+ NK cells: a functional intermediate stage of NK cell differentiation. *J Immunol*. 2011;186(12): 6753-6761.
30. Viel S, Marçais A, Guimaraes FS, et al. TGF-β inhibits the activation and functions of NK cells by repressing the mTOR pathway. *Sci Signal*. 2016;9(415): ra19.
31. Holt D, Ma X, Kundu N, Fulton A. Prostaglandin E(2) (PGE (2)) suppresses natural killer cell function primarily through the PGE(2) receptor EP4. *Cancer Immunol Immunother*. 2011;60(11):1577-1586.
32. Haraguchi K, Suzuki T, Koyama N, et al. Notch activation induces the generation of functional NK cells from human cord blood CD34-positive cells devoid of IL-15. *J Immunol*. 2009;182(10):6168-6178.
33. Robertson MJ, Caligiuri MA, Manley TJ, Levine H, Ritz J. Human natural killer cell adhesion molecules. Differential expression after activation and participation in cytolysis. *J Immunol*. 1990;145(10):3194-3201.
34. Michel T, Poli A, Cuapio A, et al. Human CD56bright NK cells: an update. *J Immunol*. 2016;196(7):2923-2931.

35. Björkström NK, Riese P, Heuts F, et al. Expression patterns of NKG2A, KIR, and CD57 define a process of CD56dim NK-cell differentiation uncoupled from NK-cell education. *Blood*. 2010;116(19):3853-3864.

36. Phillips JH, Lanier LL. A model for the differentiation of human natural killer cells. Studies on the in vitro activation of Leu-11+ granular lymphocytes with a natural killer-sensitive tumor cell, K562. *J Exp Med*. 1985;161(6):1464-1482.

37. Nielsen CM, White MJ, Goodier MR, Riley EM. Functional significance of CD57 expression on human NK cells and relevance to disease. *Front Immunol*. 2013;4:422.

38. Bryceson YT, March ME, Barber DF, Ljunggren HG, Long EO. Cytolytic granule polarization and degranulation controlled by different receptors in resting NK cells. *J Exp Med*. 2005;202(7):1001-1012.

39. Mace EM, Monkley SJ, Critchley DR, Takei F. A dual role for talin in NK cell cytotoxicity: activation of LFA-1-mediated cell adhesion and polarization of NK cells. *J Immunol*. 2009;182(2):948-956.

40. Grzywacz B, Kataria N, Verneris MR. CD56(dim)CD16(+) NK cells downregulate CD16 following target cell induced activation of matrix metalloproteinases. *Leukemia*. 2007;21(2):356-359, author reply 359.

41. Nielsen N, Ødum N, Ursø B, Lanier LL, Spee P. Cytotoxicity of CD56(bright) NK cells towards autologous activated CD4+ T cells is mediated through NKG2D, LFA-1 and TRAIL and dampened via CD94/NKG2A. *PLoS One*. 2012;7(2):e31959.

42. Leavenworth JW, Wang X, Wenander CS, Spee P, Cantor H. Mobilization of natural killer cells inhibits development of collagen-induced arthritis. *Proc Natl Acad Sci U S A*. 2011;108(35):14584-14589.

43. Park JY, Pillinger MH, Abramson SB. Prostaglandin E2 synthesis and secretion: the role of PGE2 synthases. *Clin Immunol*. 2006;119(3):229-240.

44. Martinet L, Jean C, Dietrich G, Fournié JJ, Poupot R. PGE2 inhibits natural killer and gamma delta T cell cytotoxicity triggered by NKR and TCR through a cAMP-mediated PKA type I-dependent signaling. *Biochem Pharmacol*. 2010;80(6):838-845.